Available online at www.sciencedirect.com

ScienceDirect

journal homepage: www.elsevier.com/locate/ajps

Original Research Paper

Fabrication, characterization, *in vitro* drug release and glucose uptake activity of 14-deoxy, 11, 12-didehydroandrographolide loaded polycaprolactone nanoparticles

Nagalakshmi Kamaraj, Pooja Yashwanthi Rajaguru, Praveen kumar Issac, Sujatha Sundaresan *

Department of Biotechnology, School of Bioengineering, SRM University, Kattankulathur 603203, India

ARTICLE INFO

Article history:
Received 10 August 2016
Received in revised form 24 January 2017
Accepted 15 February 2017
Available online 27 February 2017

Keywords:
Nanoencapsulation
Polycaprolactone
14-deoxy 11, 12-didehydro andrographolide
Glucose uptake
In vitro drug release
Cellular uptake

ABSTRACT

Biodegradable polymer based novel drug delivery systems brought a considerable attention in enhancing the therapeutic efficacy and bioavailability of various drugs. 14-deoxy 11, 12-didehydro andrographolide (poorly water soluble compound) loaded polycaprolactone (nano-DDA) was synthesized using the solvent evaporation technique. Nano-DDA was characterized by scanning electron microscopy (SEM) and dynamic light scattering (DLS) studies. Fourier Transform InfraRed Spectroscopy (FTIR) was used to investigate the structural interaction between the drug and the polymer. Functional characterization of the formulation was determined using drug content, cellular uptake and *in vitro* drug release. 2-deoxy-D-[1-^{3}H] glucose uptake assay was carried out to assess the antidiabetic potential of nano-DDA in L6 myotubes. The nano-DDA displayed spherical shape with a smooth surface (252.898 nm diameter), zeta potential, encapsulation and loading efficiencies of –38.9 mV, 91.98 ± 0.13% and 15.09 ± 0.18% respectively. No structural alteration between the drug and the polymer was evidenced (FTIR analysis). Confocal microscopy studies with rhodamine 123 loaded polycaprolactone nanoparticles (Rh123-PCL NPs) revealed the internalization of Rh123-PCL NPs in a time dependent manner in L6 myoblasts. A dose dependent increase in glucose uptake was observed for nano-DDA with a maximal uptake of 108.54 ± 1.42% at 100 nM on L6 myotubes, thereby proving its anti-diabetic efficacy. A biphasic pattern of *in vitro* drug release demonstrated an initial burst release at 24 h followed by a sustained release for up to 11 days. To conclude, our results revealed that nano-DDA formulation can be a potent candidate for antidiabetic drug delivery.

* *Corresponding author.* Department of Biotechnology, School of Bioengineering, SRM University, Kattankulathur 603203, India. Fax: 91-44-27452343.
E-mail address: sujatha.sa@ktr.srmuniv.ac.in (S. Sundaresan).
Peer review under responsibility of Shenyang Pharmaceutical University.
http://dx.doi.org/10.1016/j.ajps.2017.02.003

1. Introduction

Type 2 diabetes mellitus is the most prevalent form of diabetes constituting 90–95% of the diabetic population [1] and is characterized by insulin resistance. Impaired insulin secretion and free radical formation are the initial events triggering the development of insulin resistance and dysregulation of glucose and fatty acid metabolism [2]. DDA (14-deoxy-11, 12-didehydroandrographolide) is a diterpenoid of the annual herbaceous plant, *Andrographis paniculata* [3], that has been used for centuries in Asian countries to treat infections of gastrointestinal, upper respiratory tract and diseases including herpes [4]. DDA has also been proven for its potent cardiovascular effects [5], vasorelaxant effect [6], anti-diabetic nephropathy effect [7] and antidiabetic effect *in vitro* (unpublished data).

In recent years, biomaterial research led to an increased interest in the usage of biodegradable polymeric nanoparticles for hydrophobic bioactive principles in drug delivery systems. In spite of extensive research and development, these bioactive compounds did not find their way into clinical applications due to their low solubility factor. Attempts were made to encapsulate these compounds into the nanoparticulate system (liposomes, polymeric nanoparticles, lipo-nanoparticles, biodegradable microspheres, cyclodextrin, and hydrogels) to reach the target sites effectively. Nanoencapsulated drugs, fabricated with therapeutic agents, were loaded on a biodegradable polymer matrix. The diameter of these nanoparticles (NPs) ranges between 1 and 1000 nm [8]. Although various biodegradable polymers were used in the formulation of nanoencapsulation, Polycaprolactone (PCL) was highly preferred due to its biodegradability and low cost [9]. Further, PCL is achiral and renders resistance against chemical hydrolysis, which enhances the structural stability of polymeric chains in the nanoencapsulation. Due to its permissible nature to a broad range of drugs and lack of toxicity, PCL and its derivatives are well suited for colloidal drug delivery [10]. In our study, PCL was used as a biodegradable polymer for nanoencapsulation of DDA. Its physiochemical characteristics along with *in vitro* drug release were determined. To the best of our knowledge, our study is the first to report on the synthesis and anti-diabetic efficacy of nanoencapsulated DDA (nano-DDA).

2. Materials and methods

2.1. Chemicals

Polycaprolactone was purchased from Sigma-Aldrich Limited, Bangalore. 14-deoxy,11,12-didehydro andrographolide was purchased from Apeksha Research Centre Private Limited, Indore, Madyapradesh, India. Polyvinyl alcohol and Tween 20 were procured from HiMedia, Mumbai, India. All other chemicals and reagents used unless otherwise stated were of analytical grade.

2.2. Formulation of nanoencapsulation of DDA in PCL

Four formulations of nanoparticles containing PCL-DDA conjugate (A1–A4) were fabricated by solvent evaporation technique [11]. Briefly, known amounts of the DDA (Table 1) and PCL were added to 10 ml of dichloromethane, stirred to ensure that the materials were dissolved. The organic phase was introduced slowly into either 0.5% PVA (A1), 1% Tween 20 (A2 and A3), double emulsion containing 0.5% PVA or 1% Tween 20 solution (A4) resulting in an emulsion. This emulsion was broken down into nanodroplets using a Bandelin sonopuls sonicator (model UW2070, BANDELIN electronic GmbH & Co. KG, Berlin) and the nanodroplets formed nanoparticles upon evaporation. The solvent was evaporated with continuous magnetic stirring at 60 rpm under atmospheric conditions for 4 h leaving behind a colloidal suspension of nano-DDA. The nanoparticles were recovered by collecting the precipitate by centrifugation at 14,000 rpm for 15 min. The pellet was air-dried and then stored at 4 °C.

2.3. Size, morphology, PDI and zeta potential determination

SEM was used to study the shape and morphology of the nanoparticles [12]. Nano-DDA was re-suspended in sterile water, vortexed vigorously and then loaded onto a double-sided adhesive carbon tape. Samples were coated with a gold layer under vacuum for 30 s and were observed at an acceleration voltage of 5 kV. SEM image was analyzed using Image J software. Polydispersity index (PDI) was noted to determine the narrowness of the particle distribution. Zeta potential was acquired using a Zetasizer Ver. 7.11 (Malvern Instruments Ltd, UK). Sample was diluted and filtered to avoid multiscattering phenomena. The electrophoretic mobility was converted to zeta potential using the in-built software using Helmholtz–Smoluchowski equation.

2.4. Fourier Transform Infrared spectroscopy (FTIR)

FTIR analysis reveals the presence of encapsulated compound in nanoparticles by analyzing the functional groups [13]. Sample pellets were prepared by dispersing a sample (drug, polymer and nano DDA preparation) in potassium bromide and applying a pressure of 5 tons using a hydraulic press. FTIR spectra of loaded NPs were obtained using an IR spectrophotometer (Agilent Technologies, Cary 660 FTIR, USA). The same were obtained for PCL, DDA and PVA, which served as standards.

Table 1 – Optimization of PCL vs DDA ratio.

Formulation code	DDA: PCL ratio	DDA (mg)	PCL (mg)	Surfactant	Ultrasonication time (min)
A1	1:5	2	10	0.5% PVA	4
A2	1:4	2	8	1% Tween 20	3
A3	1:5	2	10	1% Tween 20	3
A4	1:5	2	10	1% Tween 20, 0.5 % PVA (double emulsion)	3 (twice)

2.5. Drug content, loading efficiency, encapsulation efficiency

The amount of drug loaded in the nanoencapsulation was determined by HPLC. Briefly, a known quantity of prepared nano-DDA (5 mg/5 ml) was subjected to pass through the column after filtration through 0.22 μ with acetonitrile:water (47:53 v/v) as mobile phase. At a flow rate of 0.5 ml/min and with an injection volume of 10 μl, the peak was detected at 263 nm. The content of DDA was calculated using the area of the principal peak by single point standardization technique [14].

To determine the amount of free DDA, the supernatant was collected at the end of the formulation by centrifugation. The absorbance was measured at 263 nm in UV Spectrophotometer using empty NPs as blank.

The encapsulation and loading efficiencies were calculated using the following formulae [15].

Encapsulation Efficiency (%)
= (Weight of initial amount of DDA – Weight of free DDA/ Weight of initial amount of DDA) × 100

Loading efficiency (%)
= Weight of initial amount of DDA – Weight of free DDA/ Total Weight of nanoparticles) × 100

2.6. In vitro release of DDA from nanoencapsulation

In vitro release of DDA from PCL matrix was estimated using a dialysis bag immersed in phosphate buffered saline (PBS; pH 7.4) [16]. Dialysis membrane of 10,000 Da cut-off was pre-treated to remove glycerol and other metal traces. A known amount of nano-DDA (A1 formulation) was dispersed in 2 ml of Phosphate buffered saline (PBS) with a pH 7.4 and introduced into the dialysis bag. The dialysis bag was immersed in 35 ml of PBS at 37 ± 0.5 °C with continuous magnetic stirring at 60 rpm. Samples were collected at regular time intervals and fresh dissolution medium of the same volume was replaced to maintain a constant volume. The amount of drug released was determined using UV spectrophotometer at 263 nm. The % release profile of free and nano-DDA were obtained by calculating the ratio of the quantity of DDA released to the total drug content in the same volume of sample.

Drug release (%) = (Released DDA/Total DDA) × 100

2.7. Mathematical modeling of the release experiments

Mechanism of drug release from the matrix is a crucial factor in determining the therapeutic potential of a drug. To describe the rate of drug release from the nanoformulation, a new mathematical model is derived. A semi-empirical model namely Korsemeyer–Peppas model was applied to the DDA release from the matrix to classify the type of mechanism involved [17]. As proposed by Korsemeyer and Peppas, the mechanism of release was characterized by release exponent (n). To demonstrate the mechanism of drug release, first 60% of drug release data were fitted in Korsemeyer–Peppas model [18].

$$M_t/M_\infty = kt^n$$

where M_t/M_∞ = fraction drug release at time 't', K = rate constant which reflects the structural and geometrical aspects of the system, and n = release exponent (which reflects the type of release mechanism).

2.8. Surfactant removal study

Residual polyvinyl alcohol present in the nanoencapsulation was determined by colorimetric method [19]. Briefly, lyophilized nanoparticles were treated with 0.5 M sodium hydroxide for 15 min at 60 °C. Samples were neutralized with 900 μl of 1N Hydrochloric acid and the volume was adjusted to 5 ml with distilled water. To the sample, 3 ml of 0.65M boric acid followed by 0.5 ml of I_2/KI (0.05M/0.15M) was added and incubated for 15 min. The absorbance was read at 690 nm and the concentration of PVA was determined using a standard plot of PVA.

2.9. Cell culture studies

L6 (rat skeletal muscle cells) were cultured in DMEM with 10% Fetal Bovine Serum (FBS) and supplemented with penicillin (120 units/ml), streptomycin (75 μg/ml), gentamycin (160 μg/ml) and amphotericin B (3 μg/ml) in a 5% CO_2 environment. For differentiation, the L6 cells were transferred to DMEM with 2% FBS for four days, post-confluence. Differentiation of L6 cells was established by observing the multinucleation of cells. The differentiated cells were incubated with high glucose medium (25 mM/l glucose) for 24 h in order to develop insulin resistance [20].

2.9.1. Cellular uptake study

Cellular uptake was determined by loading the polymer using a fluorochrome (rhodamine-123) according to Chawla and Amiji [21]. To prepare the dye-entrapped nanoparticles, rhodamine-123 was added to the polymer/dichloromethane solution; later, polyvinyl alcohol was introduced into the mixture and kept under magnetic stirring. The concentration of the fluorophore was optimized at 1.0% (w/w) of the polymer since fluorescence signal was lost due to photobleaching at lower concentrations. Since rhodamine-123 is a hydrophobic dye [22], it was efficiently loaded in the PCL nanoparticles. Rhodamine-123 containing nanoparticle suspension was prepared by re-suspending the washed pellet using de-ionized distilled water. After the washing steps, 100 μl of rhodamine-123 containing PCL nanoparticle aliquot was added to the L6 myoblast that were cultured on glass coverslips. After incubation for specific time intervals (30 min, 1 h, 2 h), the media was removed and plates were gently washed with sterile PBS. Finally, the cells were fixed with 4% paraformaldehyde and the individual coverslips were mounted on clean glass slides. Nucleus was stained using DAPI. The slides were viewed under a confocal microscope (Carl Zeiss laser scanning microscope LSM700) at 40× magnification at an excitation and emission of 500 nm/560 nm for rhodamine-123 and 358 nm/461 nm for DAPI respectively.

2.9.2. Assessment of cytotoxicity by MTT assay

The effect of the free and nanoencapsulated drug on the viability of L6 myoblast was determined by MTT (3-[4,

5-dimethylthiazol- 2-yl]-2, 5-diphenyltetrazolium bromide) assay. NAD(P)H-dependent cellular oxidoreductase enzymes are capable of reducing the yellow tetrazolium dye MTT (3-(4, 5-dimethylthiazol-2-yl)-2, 5-diphenyl tetrazolium bromide) to insoluble purple color formazan crystals. The intensity of the color is therefore directly proportional to the viability of the cells. The cell viability was calculated using the following formula [23].

$$\% \text{ Cell Viability} = (A_{570} \text{ of test}/A_{570} \text{ of control}) \times 100$$

2.9.3. *Glucose uptake assay*

L6 myotubes grown in 24-well plates (BD Falcon) were subjected to glucose uptake assay as reported [24]. Briefly, differentiated myotubes were serum starved for 5 h and were incubated with free and nano-DDA; it was then stimulated with suboptimal concentration of insulin (10 nM) for 15 min. After experimental incubation, the assay was carried out using 0.5μCi/ml of 2-deoxy-D-[1-^{3}H] glucose. The lysates were transferred to 96 well plates (Packard) and measured for cell-associated radioactivity by liquid scintillation counting. The results were expressed as counts/min and finally these data were converted to percentage of glucose uptake with respect to the untreated control. Rosiglitazone (50 μM) and Insulin (100 nM) were used as positive controls.

2.10. *Statistical analysis*

Results were expressed as mean ± SD. The data were analyzed using Graphpad Prism 5.03 statistical software (Graphad Software Inc., La Jolla, CA). The statistical significance was evaluated by one-way analysis of variance (ANOVA) and Dunnett's multiple comparison test was performed to determine significant differences between groups. The criteria for statistical significance was $P < 0.05$.

3. Results and discussion

3.1. *Formulation of polymeric nanoparticles*

The purpose of encapsulating DDA in Polycaprolactone was to develop a sustained drug release system to enable the drug to be used for antidiabetic therapy. The current study throws light on developing a safer antidiabetic therapy.

Polymer coated DDA nanoparticles were prepared by solvent evaporation method in various formulations (A1–A4) by varying the surfactants and the ultrasonification time (Table 1). At the end of the preparation, gradual evaporation of solvent led to the precipitation of the polymer and drug leading to the formation of solid shell polymeric nanoparticles with an average size of 252.898 nm (Fig. 1) for A1 formulation. Higher magnification (1200×) of the nanoparticle had shown the smooth surface with spherical shape. A2, A3 and A4 formulations showed agglomeration (sonication time, drug:polymer ratio and the type of surfactant used could influence the size and structure of the nanoparticle) [19] and hence the particle size could not be determined. Many factors play a vital role in attaining the characteristic properties of nanoparticles such as high encapsulation efficiency, small size and narrow distribution. These features of the nanoparticles have significant input in biological applications [25]. Nanoparticles possessing zeta potential above +/–30 mV are considered stable in suspension [26]. Zeta potential value and Polydispersity index (PDI) for all the formulations were tabulated. Among the four formulations, A1 formulation alone exhibited ζ potential and PDI of –38.9 ± 0.091 mV and 0.150 ± 0.002 respectively (Table 2). The results revealed that there was no aggregation due to the charge repulsion and hence considered stable in suspension (–38.9 mV). Polydispersity index <0.2 is indicative of homogenized particle size range [27]. Since the polydispersity index obtained in the study was found to be 0.150, the results revealed proper particle homogeneity. Physicochemical characteristics such as particle size and surface properties play a key role in determining the *in vitro* drug release, cellular uptake, cytotoxicity as well as their *in vivo* pharmacokinetics and biodistribution. The structural stability thereby correlates with the therapeutic efficacy of the encapsulated drug.

Table 2 – Zeta potential and Polydispersity index of nano-DDA.

Formulation	Zeta potential	Polydispersity index
A1	–38.9 ± 0.091	0.150 ± 0.002
A2	–17.30 ± 0.265	0.551 ± 0.027
A3	–15.027 ± 0.449	0.651 ± 0.029
A4	–21.067 ± 0.491	0.432 ± 0.019

Zeta potential is expressed as mV. Values are expressed as mean ± SD, n = 3.

3.2. *Drug content, drug loading and encapsulation efficiency*

The amount of drug loaded per milligram of polymer and the percentage loading was determined by re-constituting a known quantity of the nanoparticles (5 mg/5 ml) in methanol and then analyzing for the drug content by high-performance liquid chromatography (HPLC). The amount of drug loaded in the nanoencapsulation was extrapolated by calculating the area of the peak observed in the standard drug. The drug content for various formulations was tabulated (Table 3). Among the four formulations, A1 formulation showed high drug content. The amount of DDA (0.94 mg), which was encapsulated inside PCL, corroborates with the encapsulation efficiency obtained for the A1 formulation.

The nanoparticles possess the property of a high surface to volume ratio as they allow the molecules to readily incorporate as a core material. In addition, chemical nature of the compound and its polarity play a vital role in encapsulation efficiency, where the hydrophilic compounds elicit up to 10% while the hydrophobic compounds display >70% of encapsulation efficiency [17]. DDA had shown an encapsulation efficiency of 91.98 ± 0.13% which can be attributed to its hydrophobic nature. The concentration of the polymer used in the preparation was also a major determinant for encapsulation. In this study, two ratios (1:5, 1:4) were prioritized out of 5 tested ratios. From the results, it was inferred that, by increasing the polymer concentration in the organic phase, the

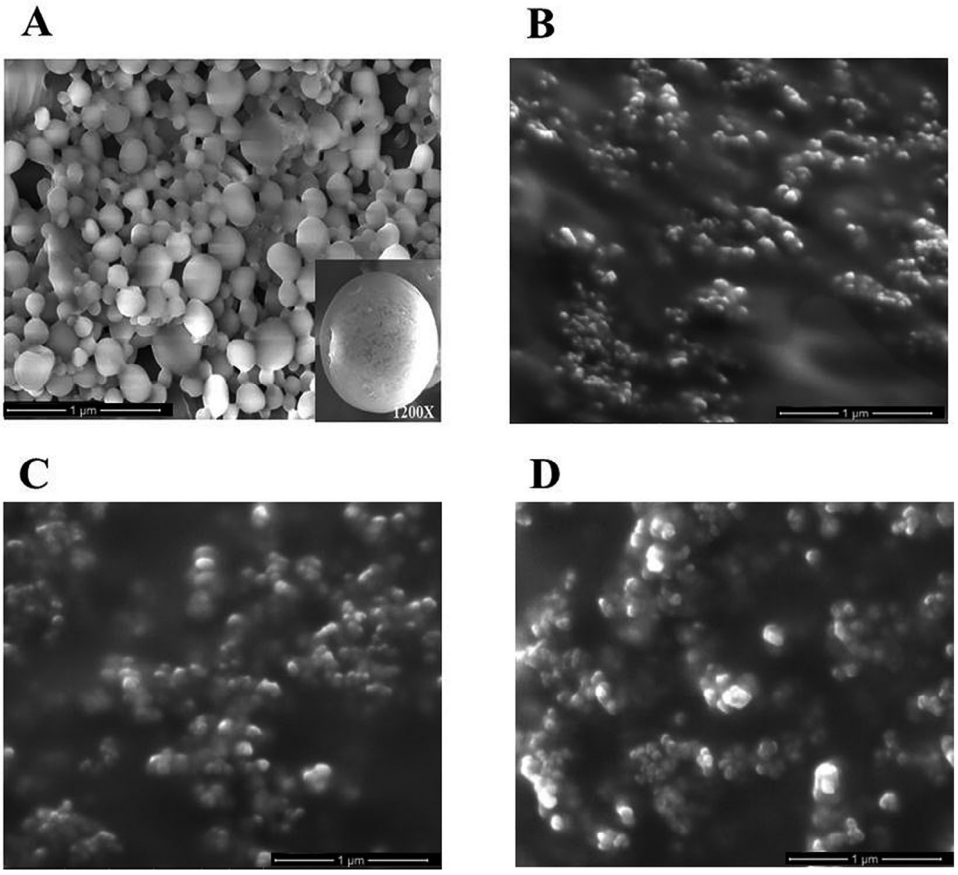

Fig. 1 – SEM images of nano-DDA [(A) A1 formulation, (B) A2 formulation, (C) A3 formulation, and (D) A4 formulation]. Scanning electron micrograph images showing surface morphology of DDA loaded PCL nanoparticles. Inset: High resolution image (1200×) of DDA loaded PCL nanoparticles.

viscosity of the solution also increased. As reported by Byun et al., the increase in viscosity can decrease the drug diffusion into the aqueous phase and thus increase the drug incorporation into the nanoparticles [28]. Consequently, the encapsulation efficiency of nanoparticles was increased upon the increase in the polymer concentration. Table 3 depicts that, among the four formulations attempted, formulation A1 has shown the highest encapsulation efficiency. Encapsulation efficiency was found to be 91.98 ± 0.13% for 1:5 ratio formulation using 0.5% PVA. The ratio of 1:5 was prioritized for future studies as the drug wastage during nanoparticle preparation was found to be minimum. The A2 and A3 formulations with Tween 20 as a surfactant and A4 formulation with the combination of Tween 20 and PVA as surfactant have shown significantly less encapsulation efficiency than A1 ($P < 0.05$). This could be attributed to the high drug wastage and a large quantity of carrier required to achieve sufficient amount of drug at target site. There was a negative proportion of loading efficiency with the encapsulation efficiency, which revealed the fact that higher loading of drug into the polymer tends to diffuse out of the matrix without exerting much biological effort. Hence, the results obtained had directed to prioritize the A1 formulation due to its high encapsulation efficiency, loading efficiency and high drug content.

Table 3 – Encapsulation, drug loading efficiencies and drug content of various formulations.

Formulation code	Encapsulation efficiency (%)	Drug loading efficiency (%)	Drug content present in 5 mg of nanoparticle (w/w)
A1	91.98 ± 0.13	15.09 ± 0.18	0.94 ± 0.015
A2	75.87 ± 0.24*	11.59 ± 0.33*	0.77 ± 0.027*
A3	52.82 ± 0.21*	10.77 ± 0.14*	0.59 ± 0.07*
A4	63.94 ± 0.23*	12.8 ± 0.26*	0.66 ± 0.025*

Values are expressed as mean ± SD, n = 3. Encapsulation and loading efficiencies were expressed in percentage. Drug content was expressed in mg. (*) $P < 0.05$ as compared with respective A1 formulation.

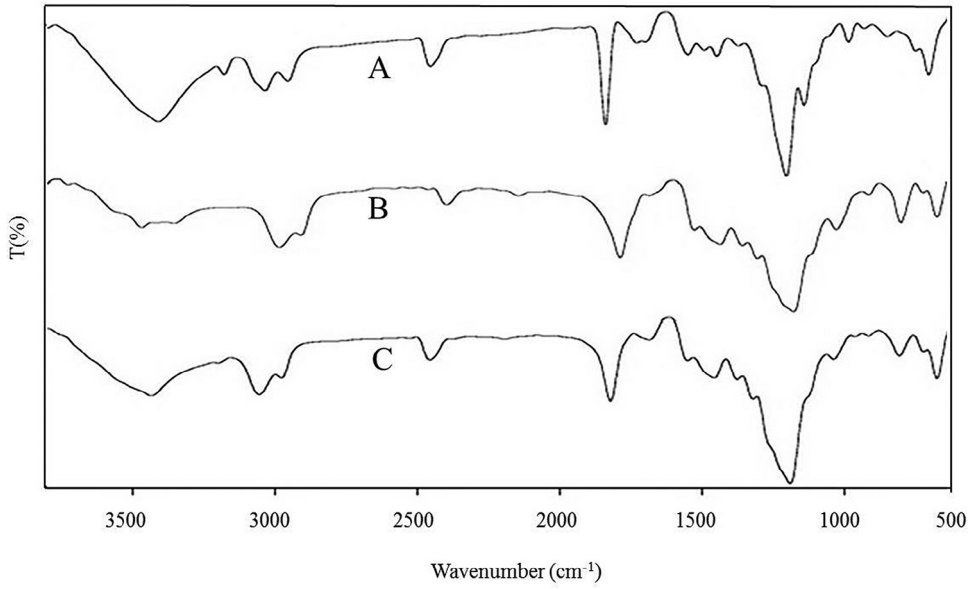

Fig. 2 – Fourier transform infrared spectroscopy (FTIR) analysis of drug, polymer and drug loaded polymer nanoparticles [(A) DDA, (B) PCL, and (C) nano-DDA].

3.3. *Fourier Transform InfraRed Spectroscopy (FTIR)*

FTIR analysis is one of the necessary tools for the quick and efficient identification of encapsulated chemical molecules [29] and much helpful in studying the chemical modifications or changes that occur in the polymer in the form of a band stretching or bending due to the addition of drug. In Fig. 2, FTIR spectra of DDA displayed a broad and main band at 3313.18/cm, corresponding to O—H stretch. Similarly, a band at 3317.77/cm was observed in spectra of nano-DDA and peak at 604.43/cm, showing similarity to the characteristic peak of DDA at 604.52/cm. In DDA, bands were observed at 1105.06/cm and at 1740.98/cm, which may be attributed to C—O and C═O stretching respectively. For PCL, bands were observed at 1112.67/cm and at 1731.36/cm, which may be attributed to C—O stretching and ketone (C═O) stretching respectively. For nano-DDA, similar peaks at 1111.53/cm for C—O stretching and 1732.09/cm and 1732.91/cm respectively for C═O stretching were observed respectively. The peaks obtained revealed that there is no significant alteration in the polymer and drug structure, thereby retaining its structural integrity. The results indicated that no alteration was observed in the functional groups of the drug and polymer, suggesting that no interaction that could interfere with polymer and drug structures were evidenced as shown in Fig. 2. The results clearly demonstrated that the configurations of functional groups present in both DDA and PCL remain unaltered, which denoted an efficient chemical stability. Similar findings for the nanoformulations with bioactive compounds have been reported earlier [16,30] in which the functional groups present in the compounds even upon encapsulation retained their configuration.

3.4. *In vitro drug release studies*

The cumulative release of DDA from PCL nanoparticles was shown in Fig. 3. A biphasic drug release pattern was evidenced by an initial release within (20% of DDA release) 24 h, which gradually increased up to 50% until 192 h, and declined at 264 h. In this study, nano-DDA passes through the pores of the dialysis membrane of lesser cut off (10,000 KDa cut off) than the PCL, hence allowing DDA to get released from the polymer matrix of the nanoparticles. The initial burst of the release of DDA was due to the immediate dissolution and release of DDA adsorbed on the surface of the nanoparticle, followed by slow and sustained release of DDA present on the core of the polymer matrix. During the study, sample aliquots were collected at predetermined intervals and the amount of DDA was quantified. The results were expressed in terms of percentage release. During the drug release process, the drug diffuses through the hydrated polymer matrix into the aqueous phase. The process of hydration relaxes the polymer chains and enhances the diffusion of drug molecules. The rate of water uptake (hydration) of copolymer particles increases with the hydrophilicity of

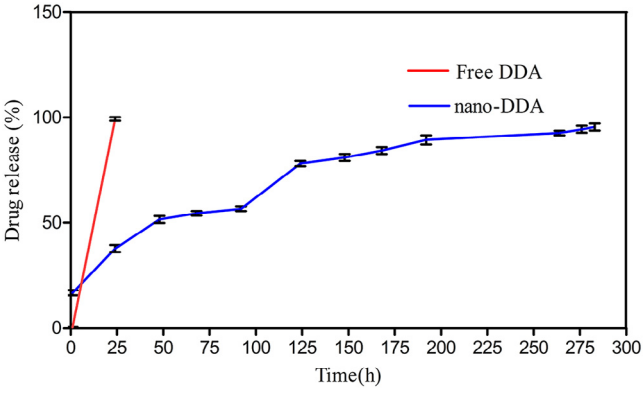

Fig. 3 – *In vitro* drug release (%) profile of DDA from PCL matrix. The values are expressed as mean ± SD of three consecutive experiments.

polymer [31]. The release profiles of DDA was monitored, as a function of time (Fig. 3) *in vitro*. Our results corroborated with the prior study reported by de la Ossa et al. in which 76–84% of cannabinoid release was at the end of day 7 from the PCL microspheres [32]. The data obtained from *in vitro* drug release studies were fitted to Korsmeyer–Peppas model (Supplementary data). The release constant (k) of the plot of log Mt/M∞ versus log t for NPs was found to be 0.3077 with the release exponent (n) value as 0.2666. Since the n value is less than 0.5, it indicates Fickian type of release [30]. However the free drug showed a fast and short release pattern from the dialysis membrane up to 24 h (Fig. 3). Hence, it was concluded that the release of DDA from NPs was carried out by Fickian diffusion.

3.5. *Cellular uptake of nanoparticles*

The analysis of intracellular uptake and its distribution were performed by incubating L6 cells with Rh-123 loaded PCL nanoparticles at specified time intervals (30 min, 1 h and 2 h) by confocal microscopy. In Fig. 4, the cells started eliciting fluorescence at 1 h (Fig. 4B) post incubation, which increased at 2 h (Fig. 4C). NPs accumulated predominantly in the cytoplasm juxtaposition in the cell membrane, thereby displaying the cellular uptake of nano-DDA. A schema of a time-dependent increase in the fluorescent signal was observed as shown in Fig. 4. Absence of any background fluorescence substantiated that the fluorescent dye loaded in the polymer did not leach out of the matrix thereby confirming the efficient loading of the dye within the polymer. The accumulation of internalization of nanoparticles was observed clearly in the cytoplasm. Our results corroborated with the prior literature reported for the cellular uptake of nanoparticles [21,33,34], in which the Rh-123 loaded nanoparticles were uptaken by the cells. Hence, the results obtained in the study substantiated the cellular uptake of the drug loaded NPs.

3.6. *Surfactant removal rate*

Due to its stabilizing nature, polyvinyl alcohol was the first surfactant studied in pharmaceutical field to prepare micro- and nano-systems [35] as an emulsion stabilizer. It has the ability to form relatively smaller nanoparticles and uniform size distribution [36]. The amount of residual PVA present in the surface of the drug–polymer matrix was determined as it may interfere with the biological applications. In our study, we observed that 92.974 ± 0.02% of residual PVA was removed efficiently by high-speed centrifugation. Our results clearly showed the efficient removal of PVA from nano-DDA. Studies have shown that nanoparticles with a lower amount of surface associated PVA showed about three-fold higher cellular uptake in vascular smooth muscle cells than the nanoparticles with higher residual PVA [19]. The residual PVA was determined to be 7.02%. However, the permissible level of PVA in a nanoformulation can be up to 13% as reported [19]; therefore, it might not interfere with the pharmaceutical application of the nano-DDA. In spite of repeated washing, a fraction of PVA might associate with the nano-DDA due to the formation of an interconnected network of the polymer at the interface [37].

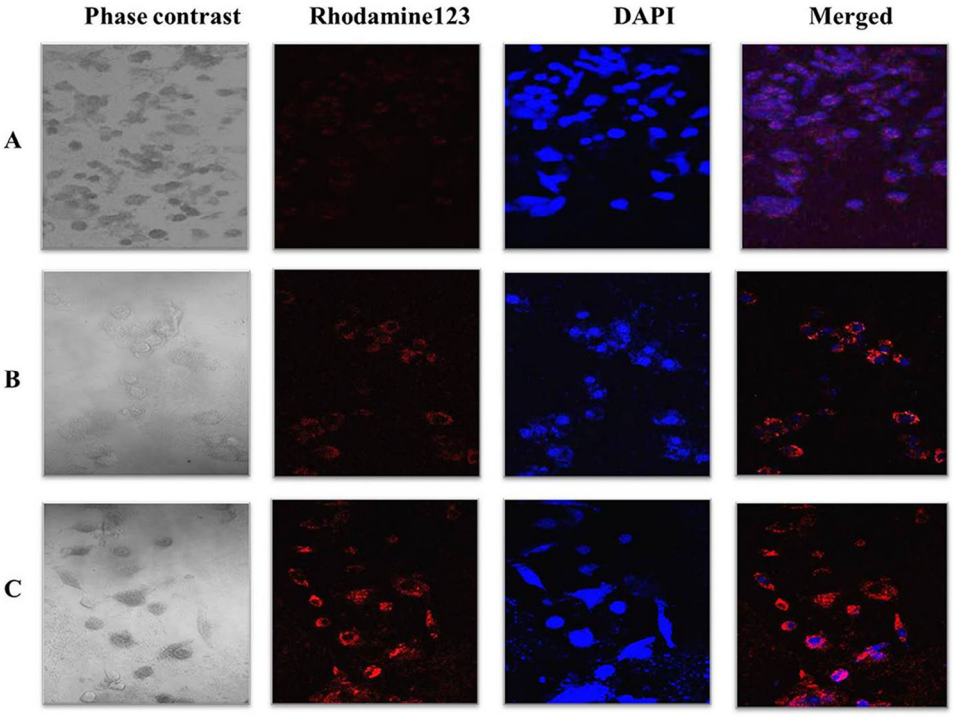

Fig. 4 – Cellular uptake of Rh-123 loaded PCL nanoparticles. Confocal microscopic images of L6 myoblast cells with Rh-123 (red) loaded PCL nanoparticles at specified time intervals: (A) 30 min, (B) 1 h, and (C) 2 h (40× magnification). DAPI (blue) was used as a nuclear stain. The merged images of Rhodamine 123 and DAPI were also shown.

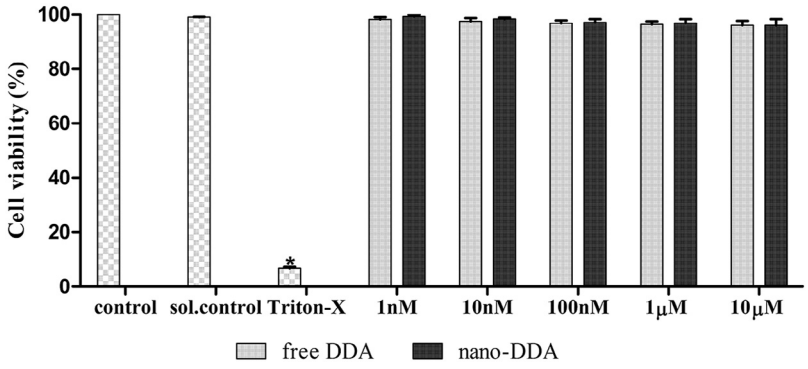

Fig. 5 – Cell viability of free DDA and nano-DDA on L6 myoblasts using MTT assay. The values are expressed as mean ± SD, n = 3 (*) $P < 0.05$ as compared with control.

3.7. *Cytotoxicity studies*

For a successful nanoformulation, it is entailed to characterize the nanoformulation and to evaluate their toxicity to reduce negative impacts on living system. To test the cytotoxic effect of the nanoformulation, cultured L6 myoblasts were exposed to various concentrations of nano-DDA. The capability of the cells in reducing MTT indicates the mitochondrial integrity and activity which could be infered as a measure of viability of cells [15]. L6 myoblasts was treated with free DDA at various concentrations to compare the cytotoxicity of free and nano-DDA. Both free and nano DDA did not alter the cell viability as shown in Fig. 5. Therefore they are found to be non-toxic up to a concentration of 10 μM. Upon treatment with free and nano-DDA, the cell viability of all the treated cells were found to be >90%, indicating that the nano-DDA and free DDA were found to be non-toxic at all tested concentrations. For both free and nano DDA, no significant cytotoxic effect was observed, which might be because DDA is a phytocompound which has been studied for various ailments [4,5,7] and Polycaprolactone was approved and utilized as a biodegradable polymer in various studies [38]. This clearly suggested that both free and nano-DDA does not pose cytotoxity to L6 myoblasts up to 10 μM.

3.8. *Glucose uptake assay*

The rationale of using L6 myotubes for studying the glucose transport has been well established [39]. The effect of free and nano DDA on 2-deoxy-D-[1-^{3}H] glucose uptake were determined to analyze their antidiabetic efficacies. The free DDA and nano-DDA exhibited an increase in glucose uptake in a dose dependent manner as depicted in Fig. 6. This dose dependent increase in glucose uptake was apparent for both free DDA and nano DDA, suggesting their significant ($P < 0.05$) antidiabetic activity. Both free and nano-DDA augmented the glucose uptake of 97.24 ± 1.44% and 108.54 ± 1.42% on par with the positive controls. Rosiglitazone and Insulin exhibited 110.0434 ± 0.21% and 125.41 ± 1.84% glucose uptake respectively. The optimum concentration exhibiting maximum glucose uptake acitivity was found to be 100 nM and 1 μM for nano-DDA and free DDA respectively. Upon nanoencapsulation, the glucose uptake activity was found to be increased as compared to free DDA. Nano-DDA was found to be on par with the positive controls used. Similarly, an increased glucose uptake >70% compared to control in L6 rat skeletal muscle cells for Epigallocatechin gallate (EGCG) was reported [40]. The nanoencapsulation of DDA resulted in an enhancement in its antidiabetic efficacy. Similarly, a gliclazide loaded alginate-methyl cellulose mucoadhesive microcapsules exhibited a significant hypoglycemic effect after 12 h of treatment to alloxan induced diabetic rats [41].

4. Conclusion

To conclude, DDA was efficiently nanoencapsulated into Polycaprolactone. The present study demonstrated a reproducible preparation of nano-DDA with spherical morphology. No significant difference was observed in the cell viability upon

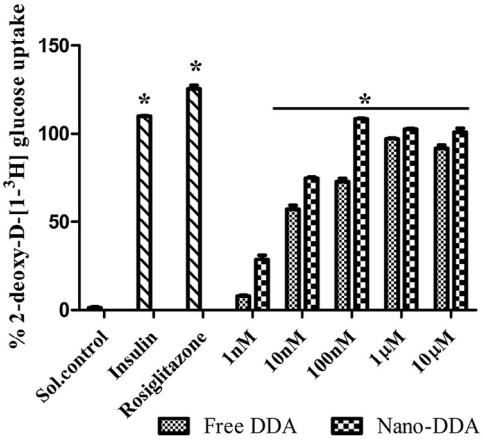

Fig. 6 – Comparative analysis of free DDA and nano-DDA on 2-deoxy-D-[1-^{3}H] glucose uptake. The results were expressed as percentage glucose uptake with respect to the control. The solvent control showed 1.36 ± 1.45% glucose uptake. The positive controls (Rosiglitazone (50 μM) and Insulin (100 nM)) exhibited 110.04 ± 0.21%, 125.41 ± 1.84% glucose uptake respectively. The values are expressed as mean ± SD, n = 3 in duplicates. (*) $P < 0.05$ as compared with control.

treatment with nano-DDA, revealing the non-toxic nature of the nanoformulation. The Rh-123 loaded PCL nanoparticles exhibited the internalization of nanoparticles. The release of DDA from polymer matrix had shown a slower, sustained and prolonged drug release from the matrix. Upon nanoencapsulation, the glucose uptake activity of the DDA was found to be enhanced due to its sustained and prolonged drug delivery. The results obtained from the study supports that the nano-DDA may serve as a potent antidiabetic compound with profound drug delivery for the treatment of diabetes. However, the exact molecular mechanism behind its antidiabetic activity needs to be elucidated.

Funding source

This research did not receive any specific grant from funding agencies in the public, commercial or not-for-profit sectors.

Acknowledgements

The authors gratefully acknowledge the Nanotechnology Research Centre (NRC), SRM University, for technical assistance in Scanning Electron Microscopy. We also thank Dr. V. Vinoth Kumar, Assistant Professor, Dept. of Biotechnology, SRM University, for his kind help in analyzing the release exponent in drug release.

Appendix: Supplementary material

Supplementary data to this article can be found online at doi:10.1016/j.ajps.2017.02.003.

REFERENCES

[1] Kumar R, Patel D, Prasad S, et al. Antidiabetic activity of alcoholic root extract of Caesalpinia digyna in streptozotocin-nicotinamide induced diabetic rats. Asian Pac J Trop Biomed 2012;2:934–940.
[2] Anand S, Muthusamy VS, Sujatha S, et al. Aloe emodin glycosides stimulates glucose transport and glycogen storage through PI3K dependent mechanism in L6 myotubes and inhibits adipocyte differentiation in 3T3L1 adipocytes. FEBS Lett 2010;584:3170–3178.
[3] Ooi JP, Kuroyanagi M, Sulaiman SF, et al. Andrographolide and 14-deoxy-11, 12-didehydroandrographolide inhibit cytochrome P450s in HepG2 hepatoma cells. Life Sci 2011;88:447–454.
[4] Sattayasai J, Srisuwan S, Arkaravichien T. Effects of andrographolide on sexual functions, vascular reactivity and serum testosterone level in rodents. Food Chem Toxicol 2010;48:1934–1938.
[5] Yoopan N, Thisoda P, Rangkadilok N, et al. Cardiovascular effects of 14-deoxy-11,12-didehydroandrographolide and Andrographis paniculata extracts. Planta Med 2007;73:503–511.
[6] Wu TS, Chern HJ, Damu AG, et al. Flavonoids and ent-labdane diterpenoids from Andrographis paniculata and their antiplatelet aggregatory and vasorelaxing effects. J Asian Nat Prod Res 2008;10:17–24.
[7] Lee MJ, Rao YK, Chen K, et al. Andrographolide and 14-deoxy-11,12-didehydroandrographolide from Andrographis paniculata attenuate high glucose-induced fibrosis and apoptosis in murine renal mesangeal cell lines. J Ethnopharmacol 2010a;132:497–505.
[8] Das RK, Kasoju N, Bora U, et al. Encapsulation of curcumin in alginate-chitosan-pluronic composite nanoparticles for delivery to cancer cells. Nanomedicine 2010;6:153–160.
[9] Mortain L, Dez I, Madec PJ. Development of new composites materials, carriers of active agents, from biodegradable polymers and wood. Comptes Rendus Chim 2004;7:635–640.
[10] Ponsart S, Coudane J, Vert M. A novel route to poly (ε-caprolactone) based copolymers via anionic derivatization. Biomacromolecules 2000;1:275–281.
[11] Mainardes RM, Evangelista RC. PLGA nanoparticles containing praziquantel: effect of formulation variables on size distribution. Int J Pharm 2005;290:137–144.
[12] Grillo R, Pereira ADES, De melo NFS, et al. Controlled release system for ametryn using polymer microspheres: preparation, characterization and release kinetics in water. J Hazard Mater 2011;186:1645–1651.
[13] Kumari A, Yadav SK, Yadav SC. Biodegradable polymeric nanoparticles based drug delivery systems. Colloids Surf B Biointerfaces 2010b;75:1–18.
[14] Cheng J, Teply BA, Sherifi I, et al. Formulation of functionalized PLGA–PEG nanoparticles for in vivo targeted drug delivery. Biomaterials 2007;28:869–876.
[15] Jain NK, Jain SK. Development and in vitro characterization of galactosylated low molecular weight chitosan nanoparticles bearing doxorubicin. AAPS PharmSciTech 2010;11:686–697.
[16] Kumar A, Sawant K. Encapsulation of exemestane in polycaprolactone nanoparticles: optimization, characterization and release kinetics. Cancer Nanotechnol 2013;4:57–71.
[17] Grillo R, Dos Santos NZP, Maruyama CR, et al. Poly (ε-caprolactone) nanocapsules as carrier systems for herbicides: physico-chemical characterization and genotoxicity evaluation. J Hazard Mater 2012;231–232:1–9.
[18] Korsmeyer RW, Gurny R, Doelker E, et al. Mechanisms of solute release from porous hydrophilic polymers. Int J Pharm 1983;15:25–35.
[19] Sahoo SK, Panyam J, Prabha S, et al. Residual polyvinyl alcohol associated with poly (D,L-lactide-co-glycolide) nanoparticles affects their physical properties and cellular uptake. J Control Release 2002;82:105–114.
[20] Sujatha S, Anand S, Sangeetha KN, et al. Biological evaluation of (3β) -STIGMAST-5-EN-3-OL as potent anti-diabetic agent in regulating glucose transport using in vitro model. Int J Diabetes Mellit 2010;2:101–109.
[21] Chawla JS, Amiji MM. Cellular uptake and concentrations of tamoxifen upon administration in poly (ε-caprolactone) nanoparticles. AAPS PharmSci 2003;5:1–7.
[22] Chawla JS, Amiji MM. Biodegradable poly (ε-caprolactone) nanoparticles for tumor-targeted delivery of tamoxifen. Int J Pharm 2002;249:127–138.
[23] Berridge MV, Herst PM, Tan AS. Tetrazolium dyes as tools in cell biology: new insights into their cellular reduction. Biotechnol Annu Rev 2005;11:127–152.
[24] Yonemitsu S, Nishimura H, Shintani M, et al. Troglitazone induces GLUT4 translocation in L6 myotubes. Diabetes 2001;12:1093–1101.

[25] Ravi Kumar MNV, Bakowsky U, Lehr CM. Preparation and characterization of cationic PLGA nanospheres as DNA carriers. Biomaterials 2004;25:1771–1777.
[26] Mohanraj VJ, Chen Y. Nanoparticles – a review. Trop J Pharm Res 2006;5:561–573.
[27] Schaffazick SR, Guterres SSU, Freitas LD, et al. Physicochemical characterization and stability of the polymeric nanoparticle systems for drug administration. Quim Nova 2003;26:726–737.
[28] Byun Y, Hwang JB, Ban SH, et al. Formulation and characterization of α-tocopherol loaded poly ε-caprolactone (PCL) nanoparticles. LWT Food Sci Technol 2011;44:24–28.
[29] Kumari A, Yadav SK, Pakade YB, et al. Development of biodegradable nanoparticles for delivery of quercetin. Colloids Surf B Biointerfaces 2010a;80:184–192.
[30] Silva MDS, Cocenza DS, Grillo R, et al. Paraquat-loaded alginate/chitosan nanoparticles: preparation, characterization and soil sorption studies. J Hazard Mater 2011;190:366–374.
[31] Budhian A, Siegel SJ, Winey KI. Controlling the in vitro release profiles for a system of haloperidol-loaded PLGA nanoparticles. Int J Pharm 2008;346:151–159.
[32] de la Ossa HP, Ligresti A, Gil-Alegre ME, et al. Poly-ε-caprolactone microspheres as a drug delivery system for cannabinoid administration: development, characterization and in vitro evaluation of their antitumoral efficacy. J Control Release 2012;161:927–932.
[33] Shah LK, Amiji MM. Intracellular delivery of saquinavir in biodegradable polymeric nanoparticles for HIV / AIDS. Pharm Res 2006;12:1–8.
[34] Nallanthighal S. Nanoencapsulation of pomegranate bioactive compounds for breast cancer chemoprevention. Int J Nanomedicine 2015;10:475–484.
[35] Pisani E, Fattal E, Paris J, et al. Surfactant dependent morphology of polymeric capsules of perfluorooctyl bromide: influence of polymer adsorption at the dichloromethane-water interface. J Colloid Interface Sci 2008;326:66–71.
[36] Mu L, Feng SS. A novel controlled release formulation for the anticancer drug paclitaxel (Taxol®): PLGA nanoparticles containing vitamin E TPGS. J Control Release 2003;86:33–48.
[37] Vimala K, Murali Mohan Y, Varaprasad K, et al. Fabrication of curcumin encapsulated Chitosan-PVA silver nanocomposite films for improved antimicrobial activity. J Biomater Nanobiotechnol 2011;2:55–64.
[38] Mahapatro A, Singh DK. Biodegradable nanoparticles are excellent vehicle for site directed in-vivo delivery of drugs and vaccines. J Nanobiotechnology 2011;9:55.
[39] Koivisto UM, Martinez-Valdez H, Bilan PJ, et al. Differential regulation of the GLUT-1 and GLUT-4 glucose transport systems by glucose and insulin in L6 muscle cells in culture. J Biol Chem 1991;266:2615–2621.
[40] Jung KH, Choi HS, Kim DH, et al. Epigallocatechin gallate stimulates glucose uptake through the phosphatidylinositol 3-kinase-mediated pathway in L6 rat skeletal muscle cells. J Med Food 2008;11:429–434.
[41] Pal D, Nayak AK. Development, optimization, and anti-diabetic activity of gliclazide-loaded alginate-methyl cellulose mucoadhesive microcapsules. AAPS PharmSciTech 2011;12:1431–1441.